Applied Catalysis B: Environmental 237 (2018) 206–213

Contents lists available at ScienceDirect

Applied Catalysis B: Environmental

journal homepage: www.elsevier.com/locate/apcatb

Catalytic reduction of bromate over catalysts based on Pd nanoparticles synthesized via water-in-oil microemulsion

Ana M. Perez-Coronado[a], Olivia Salome G.P. Soares[b], Luisa Calvo[a,*], Juan J. Rodriguez[a], Miguel A. Gilarranz[a], Manuel Fernado R. Pereira[b]

[a] Department of Chemical Engineering, C/Francisco Tomás y Valiente 7, Universidad Autónoma de Madrid, 28049, Madrid, Spain
[b] Laboratory of Catalysis and Materials (LCM) – Associate Laboratory LSRE-LCM, Faculty of Engineering, University of Porto, Rua Dr. Roberto Frias, 4200-465 Porto, Portugal

ARTICLE INFO

Keywords:
Bromate
Pd nanoparticles
Microemulsion
Reduction

ABSTRACT

Supported Pd nanoparticles (NPs) synthesized via water-in-oil (w/o) microemulsion using the water/AOT/isooctane system were used as catalysts in the bromate reduction. In order to study the influence of the support on the catalytic activity, Pd NPs were immobilized on activated carbon (AC), multi-walled carbon nanotubes (CNT) and TiO_2. Different thermal treatments in air and nitrogen were carried out in 473–673 K range to modify the supports and also to remove AOT from supported nanoparticles. The immobilization of Pd NPs on TiO_2 led to higher activity than the immobilization on the carbon-based supports. Thermal treatment of the catalysts at 673 K in air removed successfully AOT and its decomposition fragments, leading to a significant increase in activity. After removal of AOT, the experiments with catalysts prepared with Pd NPs of different size and supported on TiO_2 did not show significant differences in activity. Therefore, no evidence of structure sensitiveness was found.

1. Introduction

Bromide ion present in surface water is an increasing concern, with concentration that varies in the range from a few μg/L to several mg/L [1]. When raw water contains bromide, bromate can be generated as an ozonation byproduct in treated water [2]. Based on recent studies, bromate is classified as a “possible human” carcinogen, and drinking water standards of 10–25 μg/L are now implemented in many countries [3–5]. The lack of an efficient technology to control bromate concentration in drinking water has created a need for the development of alternatives for its removal. A wide variety of methods have been reported for the elimination of bromate in water, including filtration [6], adsorption [7], and ion exchange [8]. However, these methods simply transfer the pollutant from one phase to another and its hazards persist. Therefore, there is a niche for destructive treatment technologies that convert bromate into less toxic or innocuous end products contributing to more sustainable drinking water treatment processes [9]. Reduction processes have as main characteristics highly efficient bromate removal and stable performance over a wide pH range. Supported noble metal catalysts such as Pd, Pt, Ru and Rh efficiently promote the reduction of bromate into bromide ion under hydrogen at room temperature and pressure. Pd based catalysts are considered as the most promising among them, independently of the support used [10–12]. Pd has been identified as the “optimum” hydrogenation metal for water treatment applications [18]. A variety of supports has also been reported, including mainly activated carbon [10,13,14], alumina [11], carbon nanofibers [15–18], zeolite supported metallic catalysts [12] and titanium dioxide [19].

Restivo et al. [19] used different supports (AC, multi-walled carbon nanotubes and TiO_2) for supporting catalytic metallic phases (Pd, Pt, Rh and Ru) and exploring the catalytic reduction of bromate based on previous promising results with these catalytic systems in the reduction of nitrate [20]. It was shown that some of the supports present catalytic activity in the reduction of bromate and that the interaction of the support with the metallic phase is responsible for substantial differences in activity, finding that TiO_2 is the most active support and leads to the most active catalysts.

In the case of bromate reduction into bromide, it was proposed that the reaction mechanism on the surface of the metal comprised the dissociative adsorption of hydrogen and subsequent reaction with adsorbed bromate. Then, the bromide generated is released into the solution and the metal becomes oxidized. To complete the cycle, hydrogen also reduces the oxidized metal, which is available again to further interact with bromate and hydrogen [10]. Some catalytic

* Corresponding author.
E-mail address: luisa.calvo@uam.es (L. Calvo).

https://doi.org/10.1016/j.apcatb.2018.05.077
Received 14 February 2018; Received in revised form 21 May 2018; Accepted 27 May 2018
Available online 28 May 2018

reduction reactions with hydrogen, such as hydrodechlorination, have been reported as structure-sensitive reactions [21,22], also selectivity in nitrite reduction has been related to nanoparticles (NPs) size [23–27], but conclusive information on this is lacking for bromate reduction. The methods of synthesis that allow an accurate control of NPs size have gained much attention enabling the investigation on chemical and physical size-dependent properties. Different methods of synthesis have been reported to obtain size-controlled NPs [28–30]. Among them, the reverse microemulsion (water in oil, w/o) technique can be considered as a reproducible and flexible approach [31–35], which requires the use of water, a non-polar solvent, a reducing agent and a surfactant. Various parameters have been identified to determine the size of the NP: nature of surfactant (the length and the structure of aliphatic chain in the molecule), water to surfactant molar ratio (w_o), concentration and the type of metal precursor in water droplets, the type of reducing agent and the way of incorporating the reducing agent into microemulsion. The most important factor is the value of w_o because an increase in this ratio, while keeping other parameters constant, increases the size of formed NPs [33,36–38]. The anionic surfactant sodium bis-2-ethyl hexyl sulphosuccinate (AOT) is one of the most used surfactants. The NPs resulting from synthesis in AOT-based microeulsion systems have high stability, can have a broad range of sizes including small particles, and good monodispersity. However, the NPs may suffer from blocking due to interaction with AOT, which leads to lower values of available catalyst surface area. In previous works on the reduction of nitrite using Pd NPs synthesized using a AOT-based w/o microemulsion [21,22], we observed that the shielding effect attributed to the interaction between Pd NPs and AOT was a very interesting tool to control the selectivity to undesired product (ammonium), although at the expense of a slight reduction of the activity. It was also shown that AOT can be removed, at least partially, through thermal treatment.

The aim of this work is to evaluate the possible structure sensitiveness of the bromate reduction using Pd NPs synthesized in the AOT/isooctane reverse (water in oil) microemulsion system and immobilized on different supports as activated carbon, multi-walled carbon nanotubes and TiO_2. The methodology developed is based on the synthesis of Pd NPs with different size using the AOT/isooctane reverse (water in oil) microemulsion system, their immobilization, and the optimization of the removal of AOT from the surface of the NPs by different thermal treatments and purification methods.

2. Experimental

2.1. Material

Tetraamminepalladium (II) chloride monohydrate (≥99%, Sigma-Aldrich Co.), isooctane (99.8%, Sigma-Aldrich Co.), hydrazine hydrate solution (50–60%, Fluka) and sodium borohydride (≥ 99 9%, Sigma-Aldrich Co.) were used as received. AOT (98%, Sigma) was vacuum-dried for 24 h at 333 K immediately before use. Methanol (> 99%) and anhydrous tetrahydrofuran (≥99%) were purchased from Sigma-Aldrich Co. A commercial activated carbon (Merck), commercial multi-walled carbon nanotubes (Nanocyl NC3100) and commercial titanium dioxide (Degussa P25, 80% anatase, 20% rutile, particle size around 100 nm) were used as catalyst supports. Sodium bromate (≥ 99%, Sigma-Aldrich Co.) was used to prepare bromate solutions for the catalytic reduction experiments. Sodium bromide (≥ 99%, Sigma-Aldrich Co.) was used to prepare bromide solutions for ionic chromatography calibration. Ultrapure water was used throughout this work.

2.2. Preparation and characterization of Pd NPs

Pd NPs were synthesized by the w/o microemulsion method using the water/AOT/isooctane system. This method was selected for the preparation of nanoparticles of different size due to the high reproducibility that can be achieved, as detailed in a previous work [33]. Pd NPs were synthesized under molar water-to-surfactant ratio (w_0) values of 3, 7 and 12 in order to obtain a mean size of 6.2, 7.7 and 11.6 nm, respectively [21]. In general, a larger NP size is favoured by a lower AOT dose. The catalysts had a nominal Pd load of 1% (wt, support basis) in all cases. Three methods were used for the preparation of catalysts based on the Pd NPs synthesized.

In the first method, the Pd NPs were purified form the excess surfactant by addition of methanol followed by centrifugation. This washing procedure was repeated three times. The purified NPs were immobilised on different supports: activated carbon (AC), multi-walled carbon nanotubes (CNTs) and titanium dioxide (TiO_2). The commercial CNTs, which do not present significant surface groups [39], were subjected to different functionalization in order to obtain supports with different textural and chemical properties. CNT**s** were doped with nitrogen using melamine (M) as nitrogen precursor by ball milling of pristine CNTs with the N-precursor (CNT_M) in a Retsch MM200 equipment using the milling conditions determined in a previous work (4 h at a constant vibration frequency of 15 vibrations/s) and then the resulting material was subjected to a thermal treatment under N_2 flow at 873 K (CNT_{M_873}) [40]. Pristine CNTs were also oxidised with HNO_3 7 M during 3 h at boiling temperature to introduce oxygen-containing surface groups (CNT_{HNO3}) [39].

The following nomenclature was used for the catalysts: x/support, where x means the w_0 ratio used to synthesized the NPs and support is the type of support used. Some of the catalysts were subjected to thermal treatment during 2 h under N_2 or air atmosphere (and afterwards reduced with H_2 (473 K), and denoted as series NH and AirH (473–673 K) respectively.

In the second method, the immobilization of the Pd NPs was carried out by incorporation of the support into the microemulsion and destabilization with tetrahydrofuran (THF). In this case, Pd NPs were prepared using a w_0 value of 12. After 10 min of reduction time, the support (TiO_2) was added to the microemulsion and the mixture was stirred for 1 h. Then 150 mL of THF was added dropwise (0.25 mL/min) to destabilize the micellar medium, forcing the Pd NPs to deposit on the surface of the TiO_2. After NPs deposition, the catalyst was recovered by filtration and subsequently washed with methanol and acetone. The catalyst was recovered after washing by centrifugation and the washing procedure was repeated three times.

In the third method, the NPs were synthesized using only one microemulsion, which contained the metal precursor, using a w_0 of 12. Hydrazine (326 µL) was directly added dropwise to the microemulsion until a reductor-to-metal molar ratio of 60 was reached. After 10 min of reaction, the microemulsion was subjected to evaporation in a rotary evaporator, and then Pd NPs were washed three times with methanol. Finally, the NPs were suspended in methanol and impregnated on TiO_2 (w12/TiO_2-only-Pd ME).

Blank catalysts were prepared by incipient wetness impregnation of an aqueous solution of $PdCl_2$ using the different supports (IWI series). Prior to impregnation, the supports were degassed by ultrasonication in a low pressure system. After impregnation, the samples were dried at 373 K for 24 h, treated under 60 Ncm^3 / min N_2 flow at 473 K for 1 h, and finally reduced at 373 K under 60 Ncm^3 / min H_2 flow for 2 h [10,41].

The textural characterization of the catalysts was based on the corresponding N_2 adsorption-desorption isotherms, obtained at 77 K with a Nova 4200e (Quantachrome Instruments) equipment. The samples were degassed at 423 K during 5 h. Surface areas of the CNT samples were determined according to the Brunauer, Emmett and Teller method (S_{BET}) and the total pore volume (V_p) determined from the N_2 uptake at $p/p_0 = 0.95$.

Thermogravimetric analysis (TGA) was used as complementary technique in the study of AOT removal. The samples were heated from room temperature to 1173 K at a rate of 10 K/min in N_2 or in air. X-ray diffractograms of the samples were obtained with a Siemens model D5000 diffractometer with CuKα radiation.

The oxidation state of Pd (3d) and S (2p) core level binding was characterized by X-Ray Photoelectron Spectroscopy (XPS) using a Physical Electronics device, mod. K-Alpha equipped with an Al-Kα X-ray excitation source (1486.68 eV) (SACCS of Universidad of Extremadura). The equipment was provided by a vacuum transfer module for moving air-sensitive samples, avoiding the presence of air. Samples for XPS analysis were evaporated on an aluminum grid under N_2 atmosphere at ambient temperature to avoid oxidation. Software "XPS Peak Fit" was used for deconvolution. Peak deconvolution was performed using curves with an 80% Gaussian type and a 15% Lorentzian type and a Shirley nonlinear sigmoid-type baseline. The following peaks were used for the quantitative analysis: C 1 s, Pd 3d and S 2p. C 1 s peak (284.6 eV) was used as internal standard for binding energies. Deconvoluted peaks values are reported at NIST X- ray Photoelectron Spectroscopy Database [42].

2.3. Bromate reduction experiments

Bromate reduction runs were carried out during 2 h in a semi-batch reactor equipped with a magnetic stirrer working under vigorous stirring (700 rpm) at room temperature and atmospheric pressure. Hydrogen was used as reducing agent and it was continuously fed at 50 Ncm^3 / min flow rate. The concentration of Pd in the reaction medium was $1.25 \cdot x\ 10^{-3}$ g / L in all the reaction experiments. Initially, 790 mL of deionised water and 100 mg of catalyst were introduced into the reactor and hydrogen was fed during 15 min to remove oxygen. After this period, 10 mL of bromate solution, prepared from $NaBrO_3$, was added to the reactor, in order to obtain a concentration of 10 mg bromate/L in the reaction medium. The pH of the initial reaction medium was 5.5. Small samples were withdrawn from the reactor after defined periods of time.

The samples were analyzed by ion chromatography (Metrohm 881 Compact IC Pro) using a Metrosep A Supp 16–150.4 column and 3.6 mM Na_2CO_3 as mobile phase to determine bromate and bromide anions concentration.

A simple pseudo-first order kinetic equation was used to describe the rate of bromate disappearance. Since hydrogen is used in excess, its concentration was included into the pseudo-first-order rate constant ($k_{bromate}$) as expressed in Equation (1). The value of $k_{bromate}$ obtained by fitting of the experimental data was used to compare the activity of catalysts:

$$(-r) = \frac{-dC_{bromate}}{dt} = k_{bromate} \cdot C_{bromate} \quad (1)$$

The values of turnover frequency (TOF) were calculated and provided the number of revolutions of the catalytic cycle per unit of time and per number of active sites, and it is calculated from the first-order rate constant as follows in Eq. (2):

$$TOF\ (min^{-1}) = \frac{k_{nitrite} \cdot c_{bromate} \cdot S_{Pd} \cdot N_A}{SSA_{Pd} \cdot M_{bromate}} \quad (2)$$

where S_{Pd} is the surface occupied by one Pd-atom (0.0787 nm^2), N_A is the constant of Avogadro, SSA_{Pd} is the specific surface area of Pd avalilabe and $M_{bromate}$ is the molar mass of bromate. TOF was calculated assuming a pseudo-spherical shape of NPs and all surface sites were taken into account, thus ignoring any potential blocking of metal NPs by AOT.

3. Results and discussion

3.1. Pd NPs and catalysts characterization

The textural characterization of the prepared catalysts is shown in Table 1. As can be seen, the surface area (S_{BET}) remains practically unchanged when TiO_2 used as support. The adsorption-desorption isotherms indicate that both the supports and the catalysts are essentially non-porous and the surface area corresponds to the external surface (**Figure S1**). In the case of the catalysts supported on CNTs, significant changes in the surface area were observed after impregnation of the NPs. The changes were different depending on the treatment applied to the CNTs. The hysteresis loop observed in the adsorption-desorption isotherms corresponds to type IV, indicating that the material is mostly mesoporous (**Figure S2)**, which is explained by the free spaces in the CNT bundles. The catalysts prepared with CNT_M showed higher surface area and porosity in the whole mesopore range (Table 1, **Figure S2**) when the NPs were synthesized using high w_0 values, which can be ascribed to a lower amount of AOT remaining in the NPs after purification. In contrast, when Pd NPs were supported on CNT_{HNO3} the S_{BET} and the isotherms showed only slight changes with w_0, although a significant reduction of the surface area was observed after impregnation of the NPs. This fact shows that the functional groups on the surface of the carbon nanotubes influence the interaction with the Pd-AOT system. Pristine CNT does not present significant amount of surface groups, whereas CNT_{HNO3} presents a large amount of oxygen-containing surface groups, particularly carboxylic acids but also carboxylic anhydrides, lactones, phenols, carbonyls or quinones [39], and N-functionalities, namely quaternary nitrogen, pyridinic and pyrrole-type structures were incorporated on the carbon surface of CNT_{M_873} [40].

Table 1
Textural properties of the catalysts prepared by impregnation of Pd NPs synthesized using different w_0 values.

w_0	TiO_2	CNT_M		CNT_{M_873}		CNT_{HNO3}	
	S_{BET} (m^2/g)	S_{BET} (m^2/g)	Vp (cm^3/g)	S_{BET} (m^2/g)	Vp (cm^3/g)	S_{BET} (m^2/g)	Vp (cm^3/g)
support	50	291	1.1	338	0.87	324	0.64
3	46	171	0.53	nd	nd	248	1.53
7	47	204	0.70	nd	nd	254	1.59
12	51	284	0.73	145	0.55	214	1.45

nd: not determined.

In a previous work, dealing with the reduction of nitrite$^-$ using unsupported Pd NPs synthesized via ME with the water/AOT/isooctane system [21], we observed the difficulty to remove AOT by purification with solvents. Furthermore, in another previous work [22], we studied different thermal treatments to remove the surfactant from the catalysts surface, concluding that this treatment can increase the catalytic activity due to modification of the catalyst surface and removal of AOT. This is in agreement with the results reported by Xiong et al. [43], who observed the strong interaction of AOT with the surface of NPs and the difficulty to remove AOT due to the presence of Na and $R–SO_3^-$ in the AOT molecule.

The catalysts prepared were subjected to a thermal treatment in N_2 atmosphere (473 and 673 K) and in air (573 and 673 K) to remove AOT from the catalysts. These temperatures were select according to the decomposition range of AOT observed by TGA in air and N_2 atmosphere (**Figure S3**). Air was considered because in a previous work [22] thermal treatment in N_2 did not lead to complete removal of AOT fragments. The results shown in Table 2 indicate that, in general, the S_{BET} increases when the catalysts were treated in air. In addition, w12/CNT_{M_873} (380 m^2/g) and w12/CNT_{HNO3} (382 m^2/g) catalysts showed S_{BET} values very close to those of the original supports (CNT_{M_873}: 338 m^2/g; CNT_{HNO3}: 324 m^2/g), indicating the good removal of AOT from the catalyst. The reduction temperature was limited to 473 K in order to minimize sintering [33]. The Pd NPs in the treated catalysts can be expected to maintain substantial differences in size depending on the value of w_0 used during their synthesis.

XPS spectra were obtained in order to determine the oxidation state of Pd NPs and the changes in AOT during the thermal treatment of the catalysts [42]. Table 3 summarizes the values of d (wt. %) and Pd^{n+}/Pd° ratio obtained from the deconvolution of the 3d region

Table 2
Textural properties of the catalysts subjected to thermal treatment.

Catalyst/thermal treatment	473 K NH	673 K NH	573 K AirH	673 K AirH	
	S_{BET} (m^2/g)	S_{BET} (m^2/g)	S_{BET} (m^2/g)	S_{BET} (m^2/g)	Vp (cm^3/g)
w3/TiO_2	nd	44	nd	54	nd
w7/TiO_2	nd	nd	nd	57	nd
w12/TiO_2	nd	43	48	56	nd
w12/CNT_M	290	nd	nd	380	0.86
w12/CNT_{M_873}	nd	nd	nd	291	0.71
w12/CNT_{HNO3}	nd	nd	nd	382	1.31

nd: not determined.

spectra of Pd XPS for the catalysts synthesized via incipient wetness impregnation (IWI) and via ME and supported on TiO_2 (**Figures S4 and S5**). Pd^{n+} species were detected even in the samples subjected to reduction with hydrogen. This is a common feature of reduced Pd nanoparticles, which is ascribable to uncoordinated sites imposed by the size and morphology of the nanoparticles. Pd surface concentration was significantly higher when IWI was used to prepare catalysts, which can be due to lower agglomeration of nanoparticles and lower coverage of nanoparticles by AOT and AOT decomposition fragments. The presence of both electron deficient and zero-valent species was observed in all the catalyst series analysed [41], as it has been formerly reported for Pd catalysts and NPs prepared by different procedures [3–5]. The high Pd^{n+}/Pd° ratio observed for w3/TiO_2 can be related to the important presence of AOT, affecting not only the reduction of NPs during the synthesis but also the determination of Pd^{n+}/Pd° ratio by XPS. After thermal treatment under air or N_2 and further reduction with H_2 (w3/TiO_2_673AirH and w3/TiO_2_673NH) a substantially lower value of the Pd^{n+}/Pd° ratio can be observed. This trend can also be observed for the catalysts with NPs synthesized using a w_0 of 12.

Regarding the S species, the XPS spectra were fitted with a doublet according to NIST XPS Database (**Figure S6**) [42]. The results shown in Table 3 indicate the presence of species Pd-S, $CH_3(CH_2)S^-$, SO_3^{2-}, -C-SO_3^{2-} and metal sulphate with binding energies of 161.9, 163.6, 167.4, 168.2 and 169 eV, respectively. The catalyst based on NPs synthesized via ME showed a peak related to -C-SO_3^{2-} species, which can be associated to the R-SO_3^- head group of AOT. After thermal treatment with air, the intensity of this peak decreased and the peak associated to metal sulphate increased due to oxidation of the sample. In contrast, after the thermal treatment with N_2 the sulphate species were not detected and $CH_3(CH_2)S^-$ species were observed, which can be interpreted as fragmentation of the alkyl tails of AOT. In addition to this, Pd-S is observed, showing interaction between S and Pd.

3.2. Bromate reduction tests

As a first approach to bromate reduction, a blank test using AC, TiO_2 and CNT was carried out using H_2 (Blank H_2) and N_2 (Blank N_2) to study the role of the reducing agent and adsorption on the support. As can be seen in Fig. 1 **A**, the support without Pd NPs (Blank H_2 AC, Blank H_2 TiO_2 and Blank H_2 CNT) removes some of the bromate from the solution in the presence of H_2. This was also observed in a previous work [10] where AC was used as catalysts support for bromate reduction. Similar results were reported by Dong et al. [44] and Palomares et al. [45] when using AC and carbon nanofibers as supports, respectively. The results in Fig. 1 **A** show that under N_2 atmosphere, the bromate concentration remained nearly constant, as it was also observed by Restivo et al. [10] for TiO_2 and CNT. Thus, only minor adsorption by the support takes place and the supports contribute in some extent to the bromate reduction in the presence of H_2. On the other hand, Restivo et al. [10] observed the bromate reduction without a catalyst when H_2 was bubbled in a semi-batch system, resulting in a bromate removal of approximately 90% after 120 min of reaction.

Fig. 1**B** compares the performance of several supported catalysts prepared by different methods and unsupported Pd NPs synthesized via ME (Pd NPs, w_0 = 7). As can be seen, unsupported NPs exhibited low activity in the reduction of bromate, whereas the immobilization of the NPs on AC enhanced the activity. Nevertheless, the activity in the reduction of bromate is only slightly higher than for Pd-free supports. Likewise, the catalysts prepared by IWI showed higher activity, yielding complete bromate reduction in less than 80 min for IWI/CNT and less than 15 min for IWI/TiO_2. The interaction between bromate and TiO_2 can result in higher catalytic activity, due to electron transfer from the Ti^{3+} centres on the support lattice to the adsorbed anions [46]. A strong metal support interaction (SMSI) state can also result in the transfer of the electrons to the metallic particles [46–50]. The presence of electron enriched partially reduced species on the surface of TiO_2, which may be formed during reduction of the support, may also contribute for the reduction of anionic species. Electrostatic interaction can also have a relevant role, with the surface charge of the supports influencing the interaction with anionic species in water, thus participating in the adsorption and reaction process. While CNT supports have neutral pH (pHpzc around 7) [51], TiO_2 is slightly acidic (6) [52]. Since initial solution pH is around 5.5 and final pH is 5.0, lower than the pHpzc of both supports, a large interaction of the support's surfaces with the species in water due to surface charges may not be expected.

The influence of the support on the activity of the catalysts was studied using those with Pd NPs synthesized by ME at w_0 = 12. The results in Fig. 2 indicate that the support plays an important role. Catalysts w12/TiO_2 and w12/CNT_M exhibited higher catalytic activity during the first 30 min of reaction time; however, after this time bromate concentration decreased slowly. TiO_2 can be considered as a suitable support since has a relatively low porosity which minimize the problems of uneven distribution of the metal phase within the support. The lowest activity was observed for catalyst w12/CNT_{M_873}. This support was mechanically treated under ball-milling with the melamine and then subjected to a thermal treatment (873 K) that promotes the thermal decomposition of the N-precursor. Thus, the products released are responsible for the incorporation of N-functionalities, namely quaternary nitrogen, pyridinic and pyrrole-type structures on the carbon surface [40]. Also the catalyst w12/CNT_{HNO3} presents low activity, which must be related to the high amount of oxygen-containing groups,

Table 3
Concentration of Pd (wt. %), Pd^{n+}/Pd° ratio, S/Pd (wt. %) and contribution of S species from 2p XPS peaks for selected catalysts.

Assignment/sample	IWI/TiO_2	w3/TiO_2	w3/TiO_2_673AirH	w3/TiO_2_673NH	w12/TiO_2	w12/TiO_2_673AirH
Pd (wt., %)	3.6	0.5	1.2	1.0	1.2	1.1
Pd^{n+}/Pd°	1.3	2.85	0.36	0.06	0.57	0.24
S/Pd (wt., %)	–	9.8	3.0	3.2	2.0	2.3
Pd-S (161.9 eV)	–	–	–	12.9	–	–
$CH_3(CH_2)S^-$ (163.6 eV)	–	–	–	17.8	–	–
SO_3^{2-} (167.4 eV)	–	22.5	–	–	5.5	–
-C-SO_3^{2-} (168.2 eV)	–	72.3	53.9	69.3	81.2	63
Metal sulfate (169 eV)	–	5.2	46.1	–	13.3	37

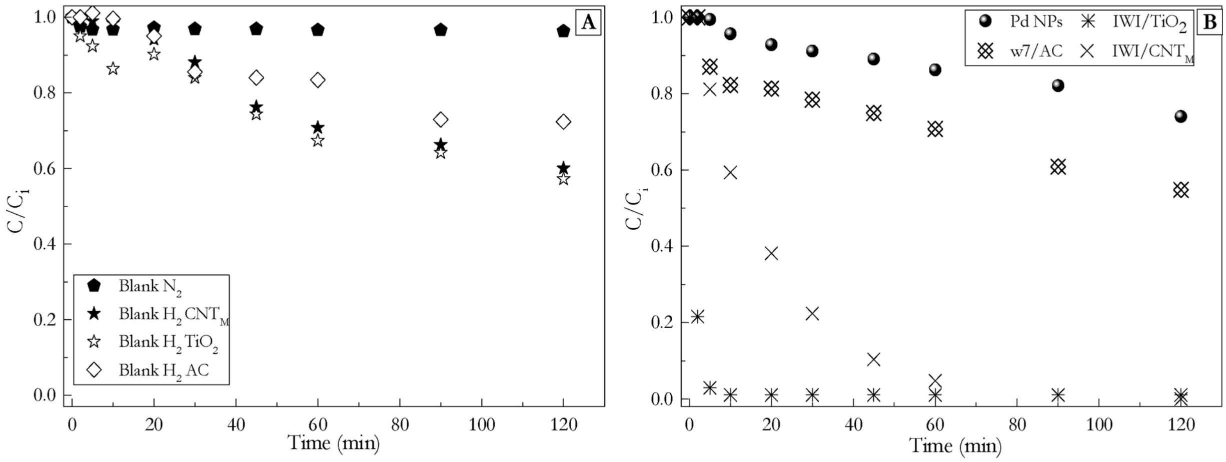

Fig. 1. Time course of dimensionless concentration for bromate reduction experiments **A)** blank experiments with Pd-free supports and **B)** Pd catalysts prepared using different procedures.

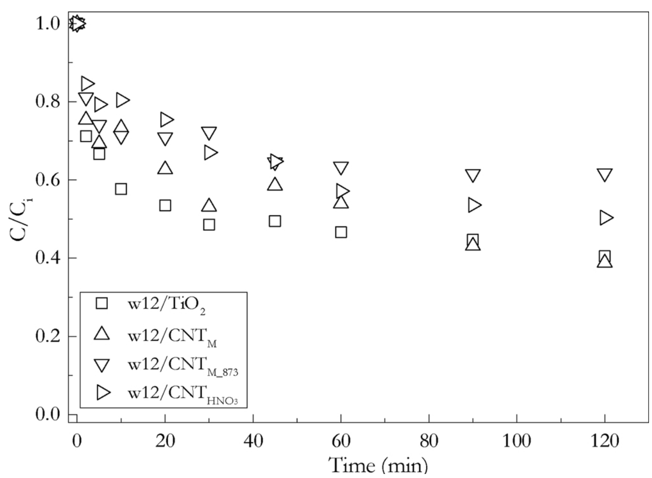

Fig. 2. Time course of dimensionless concentration for bromate reduction experiments of w12 catalyst based on different supports.

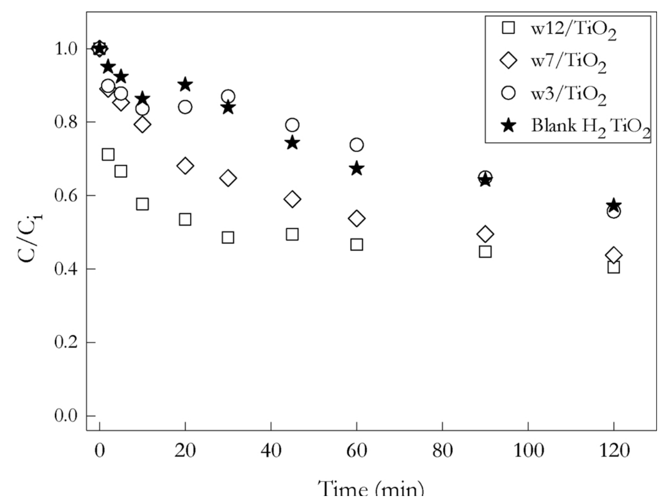

Fig. 3. Time course of dimensionless concentration for bromate reduction for catalysts prepared using different w_0 values.

mainly carboxylic acids on the carbon nanotubes surface due to oxidation in liquid phase with nitric acid [39]. On the other hand, the high activity of the catalyst w12/CNT must be related to the low amount of surface groups on the carbon nanotubes. All the catalysts prepared by ME are less active than those prepared by IWI. This performance can be due to the strong interaction between the polar group of AOT (-SO_3^-) and Pd NPs, thus producing blockage of the active phase of the catalyst and inhibition of bromate diffusion to the active centres. Additionally, the low activity observed for some of the catalysts studied can be related to a poor distribution of Pd-AOT NPs on the support due to interaction among them and agglomeration. Thus, supports with more favourable surface chemistry for the interaction with Pd-AOT NPs would lead to a higher distribution of the metal phase and a higher activity.

Catalysts with NPs synthesized with different w_0 values were supported on TiO_2 to study the effect of the Pd NPs size. This support was chosen as it showed the best performance in the former tests. It should be noted that a similar composition was estimated by XRD for all the catalysts (**Figure S7,** anatase 82–83%, rutile 18–17%). The Pd^{n+}/Pd° ratios for the catalysts synthesized by ME using w_0 values of 3 and 12 can be seen in Table 3. The results in Fig. 3 show a significant influence of the size of the Pd NPs in the bromate reduction. The Pd NPs of larger size (11.6 nm), i.e. synthesized via ME with $w_0 = 12$, led to the most active catalyst. This superior activity can be due to different factors such as i) low value of Pd^{n+}/Pd° ratio, which is in good agreement with the work of A.E. Palomares et al. [45], showing that the prevalence of Pd zero-valent species improves the bromate reduction rate, ii) lower amount of AOT coating the Pd NPs, evidenced by S/Pd ratio determined by XPS (Table 3) and iii) higher prevalence of atoms at faces and larger crystal domains in larger NPs. In this sense, these results are in agreement with those reported by Chen et al. [11] who affirm that large Pd NPs (10.2 nm) are more active than the smaller ones (9.6 nm). However, in a previous work it was reported that the catalysts based on Pd NPs synthesized via ME can exhibit an apparent structure sensitiveness due to the shielding effect of AOT [21]. This shielding could lead to lower activity in bromate reduction, and would not make possible a study of structure sensitiveness with catalysts based on Pd NPs synthesized by ME without previous removal of AOT.

To learn more on the influence of AOT and its removal on the activity of the catalysts, different thermal treatments to the catalysts were carried out. Fig. 4**A** shows the activity of catalysts based on Pd NPs ($w_0 = 12$) supported on TiO_2 and subjected to thermal treatment in air. A higher catalytic activity was obtained after the thermal treatment at 673 K than after the treatment at 573 K, suggesting higher decomposition and removal of AOT. The catalysts treated at both temperatures were more active (100% conversion, 120 min) than the one not subjected to thermal treatment ($w12/TiO_2$, 40% conversion, 120 min). Even so, they were less active than IWI/TiO2 (Fig. 1**B**).

With the aim of exploring the effect of the thermal treatment in N_2

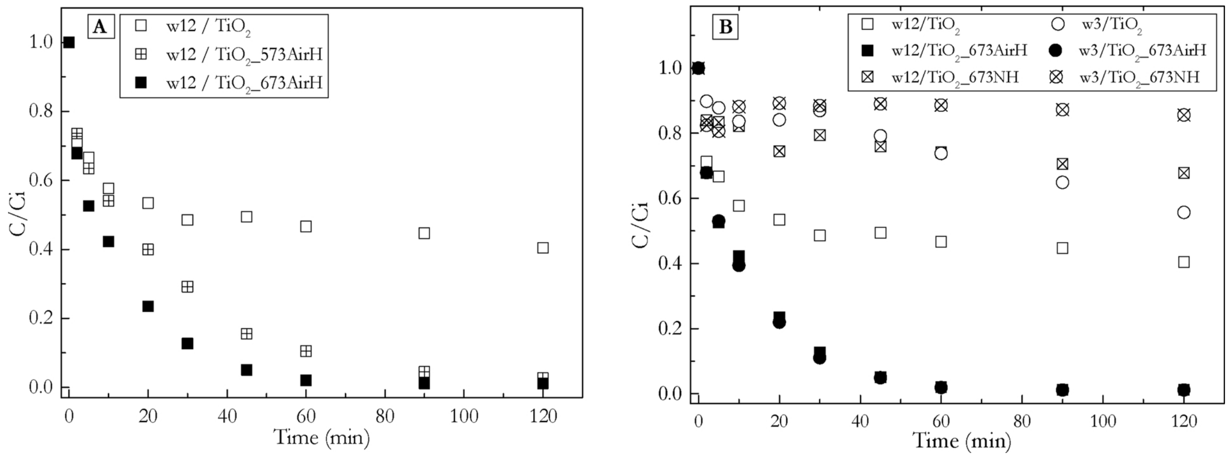

Fig. 4. Time course of dimensionless concentration for bromate during experiments using **A)** w12/TiO_2 catalysts subjected to thermal treatment in air at different temperatures followed by reduction with H_2 and **B)** catalysts subjected to thermal treatment in N_2 or air atmosphere followed by reduction with H_2.

Table 4
Kinetic parameters and TOF values of bromate reduction for catalysts synthesized with w_0 = 3 and 12 without and with thermal treatment.

Catalyst	k_{BrO3^-} 10^2 (min^{-1})	R^2	TOF 10^2 (min^{-1})
w3/TiO_2	0.5	0.952	0.11
w3/TiO_2_673AirH	7.9	0.991	1.8
w3/TiO_2_673NH	0.1	0.747	0.02
w12/TiO_2	2.9	0.939	1.2
w12/CNT_M	1.6	0.981	–
w12/CNT_{M_873}	0.3	0.956	–
w12/CNT_{HNO3}	0.8	0.971	–
w12/TiO_2_573AirH	4.5	0.992	–
w12/TiO_2_673AirH	7.8	0.993	3.3
w12/CNT_M_673AirH	6.7	0.988	–
w12/CNT_{M_873}_673AirH	2.9	0.968	–
w12/CNT_{HNO3}_673AirH	1.7	0.998	–
w12/TiO_2_673NH	0.2	0.978	0.08
w12/TiO_2 only Pd ME	1.7	0.992	–
w12/TiO_2 THF	2.3	0.996	–
w12/TiO_2 THF_673AirH	13.0	0.993	–

and in air atmosphere, catalysts synthesized with different values of w_0 (3 and 12) and supported on TiO_2 were tested. Fig. 4**B** shows that the catalysts treated in N_2 at 673 K exhibited the lowest activity in bromate reduction (Table 4). As shown by the XPS characterization (Table 3), during the thermal treatment with N_2 AOT was degraded to form alkyl chains linked to S, and the contribution of SO_3^- groups was still high after the treatment. Therefore, the strong interaction with remaining AOT and AOT decomposition products results in lower activity of the catalyst. This is in agreement with the results reported in previous studies on nitrite reduction [28], where Pd-AOT NPs subjected to thermal treatment in N_2 and H_2 showed low catalytic activity. Likewise, the catalysts with larger NPs (w_0 = 12) were more active than the one with small NPs (w_0 = 3) after the thermal treatment in N_2 atmosphere, which can be again ascribed to higher initial AOT content and higher difficulty to remove it. On the contrary, the activity of both catalysts was identical after treatment in air at 673 K, showing that after the removal of AOT, sulfonic groups and alkyl chains linked to S, the activity increases. The formation of metal sulphate species does not seem to cause loss of activity. Interestingly, after removal of AOT the catalysts with NPs synthesized using w_0 values of 3 and 12 had the same activity (Table 4), thus suggesting that the bromate reduction reaction is not structure sensitive.

After the optimization of the thermal treatment described above, the procedure was applied to catalysts based on different supports and Pd NPs synthesised using a w_0 of 12. The results obtained are presented in Fig. 5, and the corresponding kinetic parameters can be seen in Table 4.

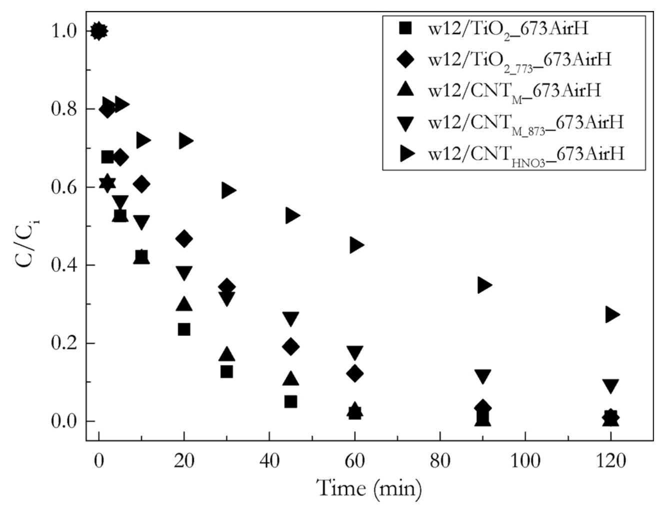

Fig. 5. Dimensionless concentration of bromate vs reaction time for catalyst based on different supports subjected to thermal treatment in air atmosphere followed by reduction with H_2.

The catalysts subjected to the optimized thermal treatment (Fig. 5) are more active than the non-treated ones (Fig. 2). Also, a better initial activity of the catalysts subjected to thermal treatment is achieved. These results are therefore consistent with those obtained using TiO_2 as support. The highest activity in bromate reduction was achieved with catalysts w12/TiO_2_$AirH_2$ and w12/CNT_M_AirH, followed by w12/TiO_{2_773}_AirH and w12/CNT_{M_873}_AirH. Catalysts based on carbon nanotubes subjected to thermal treatment with air showed the same behavior than the untreated ones. Thus, the highest catalytic activity was found for w12/CNT_M_673AirH catalyst whose support showed the lowest amount of surface groups. TOF for Pd catalysts supported on TiO_2 in bromate reduction is dependent of Pd NPs size 0.1×10^{-2} vs 1.2×10^{-2} min^{-1} for w3/TiO_2 (d = 6.2 nm) and w7/TiO_2 (11.6 nm), respectively. Apparent structure sensitiveness results from the interaction between AOT and the NPs. However, when catalysts were subjected to thermal treatment with air, differences in TOF values were much lower: 1.8×10^{-2} vs 3.3×10^{-2} min^{-1} for w3/TiO_2_673AirH and w12/TiO_2_673AirH catalysts, respectively. The difference between these values are of low significance and suggests that the bromate reduction reaction may not be structure sensitive.

To improve the understanding of the effect of AOT on the activity of the catalysts, the influence of the NPs preparation method was studied. As can be seen in Fig. 6, the catalyst w12/TiO_2 THF was more active than the others. Pd NPs were supported using THF as destabilizing in

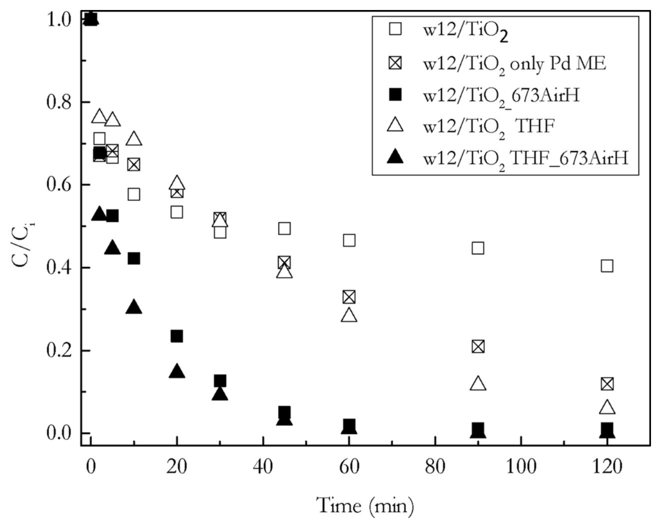

Fig. 6. Time course of dimensionless concentration for bromate reduction experiments for catalysts purified using different techniques.

the presence of the support, which can avoid the agglomeration of NPs and lead to a better distribution on the support and improved activity. The use of THF as destabilizing agent and the corresponding enhancement of the interaction with the support has been reported by others [53,54]. Nevertheless, catalyst w12/TiO_2 THF was less active than w12/TiO_2_673AirH, probably because THF is a destabilizing agent but it does not contribute to the complete removal of AOT.

Finally, w12/TiO_2 THF catalyst was treated at 673 K in air and then reduced with H_2 in order to combine the methods described above. As can be seen in Fig. 6 and Table 4, this catalyst shows the highest activity in the reduction of bromate. However, it has to be noted that the activity only improved slightly in comparison to w12/TiO_2_673AirH catalyst, thus showing that the treatment in air is itself very effective in the removal of AOT and in the enhancement of the activity.

4. Conclusions

A detailed study on the influence of the Pd NPs synthesis by the ME method supported on different materials (AC, TiO_2 and CNT) as catalysts for the bromate reduction with H_2 in water was carried out. The best activity results were observed for the catalysts supported on CNT and TiO_2. A lower reaction time was observed for Pd NPs synthesized with w_0 equal to 3. These catalysts showed a higher amount of AOT on the catalysts surface, which led to lower catalytic activity. When catalyst NPs synthesized using w_0 equal to 3 and 12 were subjected to a thermal treatment under air, an increase in activity leading to complete reduction of bromate was achieved as a result of the AOT removal. Besides, the destabilization of Pd NPs ME with THF also proved to be a good procedure to remove AOT. Finally, when this purification procedure was combined with thermal treatment with air, the highest activity in bromate reduction was achieved. The results for the catalysts based on NPs of different size free from AOT suggest that bromate reduction is not a structure sensitive reaction.

Acknowledgements

This work is a result of project “AIProcMat@N2020 - Advanced Industrial Processes and Materials for a Sustainable Northern Region of Portugal 2020”, with the reference NORTE-01-0145-FEDER-000006, supported by Norte Portugal Regional Operational Programme (NORTE 2020), under the Portugal 2020 Partnership Agreement, through the European Regional Development Fund (ERDF) and of Project POCI-01-0145-FEDER-006984 – Associate Laboratory LSRE-LCM funded by ERDF through COMPETE2020 - Programa Operacional Competitividade e Internacionalização (POCI) – and by national funds through FCT - Fundação para a Ciência e a Tecnologia. The authors also greatly appreciate financial support from the Spanish MINECO (CTQ2012-32821 and CTQ2015-65491-R).

Appendix A. Supplementary data

Supplementary material related to this article can be found, in the online version, at doi:https://doi.org/10.1016/j.apcatb.2018.05.077.

References

[1] Q. Xiao, Y. Ren, S. Yu, Pilot study on bromate reduction from drinking water by UV/sulfite systems: economic cost comparisons, effects of environmental parameters and mechanisms, Chem. Eng. J. 330 (2017) 1203–1210.
[2] R. Hofmann, R.C. Andrews, Potential side effects of using ammonia to inhibit bromate formation during the ozonation of drinking water, J. Environ. Eng. Sci. 6 (2007) 739–743.
[3] M. Naushad, Z.A. Alothman, M.R. Khan, S.M. Wabaidur, Removal of bromate from water using de-acidite FF-IP resin and determination byultra-performance liquid chromatography-tandem mass spectrometry, Clean Soil Air Water 41 (2013) 528–533.
[4] U.S. EPA, National primary drinking water regulations: stage 2 disinfectants and disinfection byproducts rule, Fed. Regist. 71 (2006) 387–493.
[5] H. Noguchi, A. Nakajima, T. Watanabe, K. Hashimoto, Design of aphotocatalyst for bromate decomposition: surface modification of TiO_2 bypseudo-boehmite, Environ. Sci. Technol. 37 (2003) 153–157.
[6] K. Listiarini, J.T. Tor, D.D. Sun, J.O. Leckie, Hybrid coagulation-nanofiltration membrane for removal of bromate and humic acid in water, J. Membr. Sci. 365 (2010) 154–159.
[7] A. Bhatnagar, Y. Choi, Y. Yoon, Y. Shin, B.-H. Jeon, J.-W. Kang, Bromate removal from water by granular ferric hydroxide (GFH), J. Hazard. Mater. 170 (2009) 134–140.
[8] J.A. Wisniewski, M. Kabsch-Korbutowicz, Bromate removal in the ion-exchange process, Desalination 261 (2010) 197–201.
[9] X. Chen, X. Huo, J. Liu, Y. Wang, C.J. Werth, T.J. Strathmann, Exploring beyond palladium: catalytic reduction of aqueous oxyanion pollutants with alternative platinum group metals and new mechanistic implications, Chem. Eng. J. 313 (2017) 745–752.
[10] J. Restivo, O.S.G.P. Soares, J.J.M. Órfão, M.F.R. Pereira, Metal assessment for the catalytic reduction of bromate in water under hydrogen, Chem. Eng. J. 263 (2015) 119–126.
[11] H. Chen, Z. Xu, H. Wan, J. Zheng, D. Yin, S. Zheng, Aqueous bromate reduction by catalytic hydrogenation over Pd/Al_2O_3 catalysts, Appl. Catal. B 96 (2010) 307–313.
[12] C.M.A.S. Freitas, O.S.G.P. Soares, J.J.M. Orfao, A.M. Fonseca, M.F.R. Pereira, I.C. Neves, Highly efficient reduction of bromate to bromide over mono and bimetallic ZSM5 catalysts, Green Chem. 17 (2015) 4247–4250.
[13] M.J. Kirisits, V.L. Snoeyink, J.C. Kruithof, The reduction of bromate by granular activated carbon, Water Res. 34 (2000) 4250–4260.
[14] J. Restivo, O.S.G.P. Soares, J.J.M. Órfão, M.F.R. Pereira, Bimetallic activated carbon supported catalysts for the hydrogen reduction of bromate in water, Catal. Today 249 (2015) 213–219.
[15] D.B. Thakur, R.M. Tiggelaar, Y. Weber, J.G.E. Gardeniers, L. Lefferts, K. Seshan, Ruthenium catalyst on carbon nanofiber support layers for use in silicon-based structured microreactors. Part II: catalytic reduction of bromate contaminants in aqueous phase, Appl. Catal. B 102 (2011) 243–250.
[16] Y. Marco, E. García-Bordejé, C. Franch, A.E. Palomares, T. Yuranova, L. Kiwi-Minsker, Bromate catalytic reduction in continuous mode using metal catalysts supported on monoliths coated with carbon nanofibers, Chem. Eng. J. 230 (2013) 605–611.
[17] A.E. Palomares, C. Franch, T. Yuranova, L. Kiwi-Minsker, E. García-Bordeje, S. Derrouiche, The use of Pd catalysts on carbon-based structured materials for the catalytic hydrogenation of bromates in different types of water, Appl. Catal. B 146 (2014) 186–191.
[18] P. Yaseneva, C.F. Marti, E. Palomares, X. Fan, T. Morgan, P.S. Perez, M. Ronning, F. Huang, T. Yuranova, L. Kiwi-Minsker, Efficient reduction of bromates using carbon nanofibre supported catalysts: experimental and a comparative life cycle assessment study, Chem. Eng. J. 248 (2014) 230–241.
[19] J. Restivo, O.S.G.P. Soares, J.J.M. Órfão, M.F.R. Pereira, Catalytic reduction of bromate over monometallic catalysts on different powder and structured supports, Chem. Eng. J. 309 (2017) 197–205.
[20] O.S.G.P. Soares, J.J.M. Órfão, M.F.R. Pereira, Nitrate reduction in water catalysed by Pd–Cu on different supports, Desalination 279 (2011) 367–374.
[21] A.M. Perez-Coronado, L. Calvo, J.A. Baeza, J. Palomar, L. Lefferts, J.J. Rodriguez, M.A. Gilarranz, Metal-surfactant interaction as a tool to control the catalytic selectivity of Pd catalysts, Appl. Catal. A 529 (2017) 32–39.
[22] A.M. Perez-Coronado, J.A. Baeza, L. Calvo, J. Palomar, L. Lefferts, J.J. Rodriguez, M.A. Gilarranz, Selective reduction of nitrite to nitrogen with carbon-supported Pd-AOT nanoparticles, Ind. Eng. Chem. Res. 56 (41) (2017) 11745–11754.
[23] M.A. Keane, G. Pina, G. Tavoularis, The catalytic hydrodechlorination of mono-, di- and trichlorobenzenes over supported nickel, Appl. Catal. B 48 (2004) 275–286.
[24] S. Ordóñez, E. Díaz, R.F. Bueres, E. Asedegbega-Nieto, H. Sastre, Carbon nanofibre-

supported palladium catalysts as model hydrodechlorination catalysts, J. Catal. 272 (2010) 158–168.
[25] E. Diaz, A.F. Mohedano, J.A. Casas, L. Calvo, M.A. Gilarranz, J.J. Rodriguez, Comparison of activated carbon-supported Pd and Rh catalysts for aqueous-phase hydrodechlorination, Appl. Catal. B 106 (2011) 469–475.
[26] J.A. Baeza, L. Calvo, M.A. Gilarranz, A.F. Mohedano, J.A. Casas, J.J. Rodriguez, Catalytic behavior of size-controlled palladium nanoparticles in the hydrodechlorination of 4-chlorophenol in aqueous phase, J. Catal. 293 (2012) 85–93.
[27] J.A. Baeza, L. Calvo, M.A. Gilarranz, J.J. Rodriguez, Effect of size and oxidation state of size-controlled rhodium nanoparticles on the aqueous-phase hydrodechlorination of 4-chlorophenol, Chem. Eng. J. 240 (2014) 271–280.
[28] A. Gniewek, A.M. Trzeciak, J.J. Ziółkowski, L. Kępiński, J. Wrzyszcz, W. Tylus, Pd-PVP colloid as catalyst for Heck and carbonylation reactions: TEM and XPS studies, J. Catal. 229 (2005) 332–343.
[29] K. Okitsu, H. Bandow, Y. Maeda, Y. Nagata, Sonochemical preparation of ultrafine palladium particles, Chem. Mater. 8 (1996) 315–317.
[30] P. Yong, N.A. Rowson, J.P.G. Farr, I.R. Harris, L.E. Macaskie, Bioreduction and biocrystallization of palladium by Desulfovibrio desulfuricans NCIMB 8307, Biotechnol. Bioeng. 80 (2002) 369–379.
[31] J.N. Solanki, R. Sengupta, Z.V.P. Murthy, Synthesis of copper sulphide and copper nanoparticles with microemulsion method, Solid State Sci. 12 (2010) 1560–1566.
[32] J. Bedia, L. Calvo, J. Lemus, A. Quintanilla, J.A. Casas, A.F. Mohedano, J.A. Zazo, J.J. Rodriguez, M.A. Gilarranz, Colloidal and microemulsion synthesis of rhenium nanoparticles in aqueous medium, Colloids Surf. A Physicochem. Eng. Asp. 469 (2015) 202–210.
[33] A.M. Perez-Coronado, L. Calvo, N. Alonso-Morales, F. Heras, J.J. Rodriguez, M.A. Gilarranz, Multiple approaches to control and assess the size of Pd nanoparticles synthesized via water-in-oil microemulsion, Colloids Surf. A Physicochem. Eng. Asp. 497 (2016) 28–34.
[34] H. Gustafsson, S. Isaksson, A. Altskär, K. Holmberg, Mesoporous silica nanoparticles with controllable morphology prepared from oil-in-water emulsions, J. Colloid Interface Sci. 467 (2016) 253–260.
[35] R. Kosydar, M. Góral, J. Gurgul, A. Drelinkiewicz, The effect of support properties in the preparation of Pd size-controlled catalysts by “water-in-oil” microemulsion method, Catal. Commun. 22 (2012) 58–67.
[36] I. Capek, Preparation of metal nanoparticles in water-in-oil (w/o) microemulsions, Adv. Colloid Interface Sci. 110 (2004) 49–74.
[37] J. Eastoe, M.J. Hollamby, L. Hudson, Recent advances in nanoparticle synthesis with reversed micelles, Adv. Colloid Interface Sci. 128–130 (2006) 5–15.
[38] M.A. Lopez-Quintela, C. Tojo, M.C. Blamco, L. Garcia Rio, J.R. Leis, Microemulsion dynamics and reactions in microemulsions, Curr. Opin. Colloid Interface Sci. 9 (2004) 264–278.
[39] O.S.G.P. Soares, J.J.M. Órfão, M.F.R. Pereira, Pd-Cu and Pt-Cu catalysts supported on carbon nanotubes for nitrate reduction in water, Ind. Eng. Chem. Res. 49 (2010) 7183–7192.
[40] O.S.G.P. Soares, R.P. Rocha, A.G. Gonçalves, J.L. Figueiredo, J.J.M. Órfão, M.F.R. Pereira, Easy method to prepare N-doped carbon nanotubes using ball milling, Carbon 91 (2015) 114–121.
[41] O.S.G.P. Soares, C.M.A.S. Freitas, A.M. Fonseca, J.J.M. Órfão, M.F.R. Pereira, I.C. Neves, Bromate reduction in water promoted by metal catalysts prepared over faujasite zeolite, Chem. Eng. J. 291 (2016) 199–205.
[42] M.X.- Ray, Photoelectron Spectroscopy Database 20, Version 3.0, National, Institute of Standards and Technology, Gaithersburg, 2015 (n.d.), http://srdata.nist.gov/XPS.
[43] L. Xiong, T. He, Synthesis and characterization of ultrafine tungsten and tungsten oxide nanoparticles by a reverse microemulsion-mediated method, Chem. Mater. 18 (2006) 2211–2218.
[44] Z. Dong, W. Dong, F. Sun, R. Zhu, F. Ouyang, Reaction kinetics, mechanisms and catalysis, React. Kinet. Mech. Catal. 107 (2012) 213–244.
[45] A.E.E. Palomares, C. Franch, T. Yuranova, L. Kiwi-Minsker, E. García-Bordeje, S. Derrouiche, The use of Pd catalysts on carbon-based structured materials for the catalytic hydrogenation of bromates in different types of water, Appl. Catal. B 146 (2014) 186–191.
[46] J. Sá, T. Berger, K. Föttinger, A. Riss, J.A. Anderson, H. Vinek, Can TiO_2 promote the reduction of nitrates in water? J. Catal. 234 (2005) 282–291.
[47] W.J. Kim, J.H. Kang, I.Y. Ahn, S.H. Moon, Effect of potassium addition on the properties of a TiO_2 - modified Pd catalyst for the selective hydrogenation of acetylene, Appl. Catal. A 268 (2004) 77–82.
[48] R. Green, P. Morrall, M. Bowker, CO Spillover and oxidation on Pt/TiO_2, Catal. Lett. 98 (2004) 129–133.
[49] P. Weerachawanasak, P. Praserthdam, M. Arai, J. Panpranot, A comparative study of strong metal-support interaction and catalytic behavior of Pd catalysts supported on micron- and nano- sized TiO_2 in liquid-phase selective hydrogenation of phenylacetyleneJ, Mol. Catal. A: Chem. 279 (2008) 133–139.
[50] M.S. Kim, S.-H. Chung, C.J. Yoo, M.S. Lee, I.H. Cho, D.W. Lee, K.Y. Lee, Catalytic reduction of nitrate in water over Pd–Cu/TiO_2 catalyst: effect of the strong metal-support interaction (SMSI) on the catalytic activity, Appl. Catal. B 142–143 (2013) 354–361.
[51] A.G. Gonçalves, J.L. Figueiredo, J.J.M. Órfão, M.F.R. Pereira, Influence of the surface chemistry of multi-walled carbon nanotubes on their activity as ozonation catalysts, Carbon 48 (2010) 4369–4381.
[52] M. Janus, A.W. Morawski, New method of improving photocatalytic activity of commercial Degussa P25 for azo dyes decomposition, Appl. Catal. B 75 (2007) 118–123.
[53] M. Bonarowska, Z. Karpinski, R. Kosydar, T. Szumelda, A. Drelinkiewicz, Hydrodechlorination of CCl_4 over carbon-supported palladium-gold catalysts prepared by the reverse “water-in-oil” microemulsion method, Comptes Rendus Chim. 18 (2015) 1143–1151.
[54] M. Trépanier, A.K. Dalai, N. Abatzoglou, Synthesis of CNT-supported cobalt nanoparticle catalysts using a microemulsion technique: role of nanoparticle size on reducibility, activity and selectivity in Fischer-Tropsch reactions, Appl. Catal. A 374 (2010) 79–86.